Agglomeration during Precipitation: II. Mechanism Deduction from Tracer Data

D. Ilievski and M. J. Hounslow
Dept. of Chemical Engineering, University of Cambridge, Cambridge CB2 3RA, U.K.

A novel approach using a 2-D population balance model is developed and applied to the analysis of experimental tracer crystal data. This approach is effective in discriminating among various functional forms of agglomeration kernel and enables estimation of the agglomeration kinetics. At present, the analysis is restricted to three simple agglomeration kernels and shows that the size-independent kernel best describes the agglomeration of $Al(OH)_3$ crystals during precipitation in caustic aluminate solutions. This agrees with the findings of Ilievski and White (1994). Estimates of the agglomeration kinetic parameters from the tracer data agree well with the experimentally observed values.

Introduction

In Part I, Ilievski and White (1995) describe the development and application of tracer crystals to the study of $Al(OH)_3$ precipitation mechanisms. These tracer crystals contain detectable amounts of Zn and have the crystal structure of the gibbsite polymorph of $Al(OH)_3$, the polymorph observed in industrial Bayer precipitation. The tracer crystals were demonstrated to behave in the same manner during precipitation as the nontracer $Al(OH)_3$ crystals. This article describes a novel technique for analyzing the experimental tracer data. The technique makes use of a two-dimensional (2-D) population balance and provides a useful tool to aid identification of agglomeration mechanisms. At this stage, the analysis is restricted to three simple agglomeration kernels. However, the principle can readily be extended to more complex agglomeration models if numerical, rather than analytical, techniques are used.

Several agglomeration studies in batch precipitation have been conducted on this system. To the best of our knowledge, only the study of Ilievski and White (1994) addresses the so-called *inverse problem*, where the agglomeration mechanism is inferred from the experimental particle-size distribution (PSD) data. The $Al(OH)_3$ agglomeration study of Halfon and Kaliaguine (1976) assumed *a priori* size-independent agglomeration. The study of Ilievski and White (1994) showed that $Al(OH)_3$ agglomeration could be satisfactorily modeled by a *random coalescence*, or size-independent, agglomeration mechanism. They draw this conclusion from two separate experimental results: (1) from considerations of the shape of the self-preserving PSD in batch experiments and; (2) from statistical comparisons between the quality of fit to experimental PSD data by different agglomeration models.

Experimental

The crystal tracer experiments reported here are analogous to the tracer techniques well established for the investigation of chemical reactors. The experimental details may be found in Ilievski and White (1995). A brief description of the experimental method follows. An impulse of tracer crystals of the same size as the seed is added to a crystallizer operating at steady state. Slurry samples are taken from the crystallizer product stream at different times, after the addition of the tracer. The distribution of Zn-doped tracer particles with size and time is monitored.

Tracer studies were performed on three separate continuous precipitation experiments identified as: Con7#, Con8#, and Con9#. The operating conditions are given in Table 1. The index of aggregation, I_{Agg}, by the definition of Hounslow (1990) is:

$$I_{Agg} = 1 - \frac{N_t}{N_0} \tag{1}$$

where N_t and N_0 are the total particle numbers at steady state and numbers added as seed, respectively. This quantity is an indicator of the extent of agglomeration in the crystallizer.

Current address of D. Ilievski: Hydrometallurgy, CSIRO Division of Minerals, P.O. Box 90, Bentley, Perth, WA 6151, Australia.
Correspondence concerning this article should be addressed to M. J. Hounslow.

Table 1. Operating Conditions and Results from the Precipitation Experiments

Run Identifier	Con7#	Con8#	Con9#
I_{Agg}	0.53	0.56	0.44
Seed-Size Distribution	$L_{30} = 16\ \mu m$ $\sigma \approx 2.5\ \mu m$	$L_{30} = 11.5\ \mu m$ $\sigma \approx 1.5\ \mu m$	$L_{30} = 16\ \mu m$ $\sigma \approx 2.5\ \mu m$
Supersaturation, S	0.48	0.42	0.42
Mean Res. Time, τ	67 min	59 min	47 min

In the current work N_t and N_0 are determined from particle counts with an Elzone particle sizer. Separate experiments show that the seeds do not rupture on entry to the vessel. It is well established that nucleation does not occur under the conditions reported here. It follows that both N_t and N_o, and thus I_{Agg} are well characterized experimentally.

The values of I_{Agg} in Table 1 show the presence of substantial degrees of agglomeration. Scanning electron micrographs of the steady-state product crystals from the experiments also showed evidence of agglomeration.

Quantitative Analysis of Tracer Data

Theory of the analysis technique

The experimental tracer data constitute a 2-*D* size distribution. In Appendix A we develop a 2-D population balance in terms of a particle's volume, v, and the mass of tracer it contains, c. We use this population balance to develop expressions for:

- The index of aggregation, I_{Agg}.
- The one-dimensional (1-D) population balance describing the particle-size distribution by its population density function, $n(v)$, and its associated moments, m_i.
- The mass density of tracer, $M(t, v)$, that describes the distribution of tracer mass with size, so that the mass of tracer, per unit volume of suspension, contained within particles of $v \in (v, v + dv)$, is $dm_T = M(t, v)dv$.
- The total mass of tracer per unit volume of suspension, $M_T(t) = \int_o^\infty M(t, v)dv$.
- The volume mean size of the tracer mass distribution, $\bar{v}_T(t)$, the mean of M. As will be demonstrated, the expression for $\bar{v}_T(t)$ provides a tool to aid in the identification of the agglomeration mechanism.

The analysis presented in Appendix A is possible for only a limited set of idealized conditions. The assumptions are now presented and their validity discussed. In all cases we assume that:

(1) *Size Enlargement Occurs Only by Aggregation.* Earlier batch precipitation experiments on this system (Ilievski and White, 1994) show that the kinetics of growth from solution are slow compared to the agglomeration kinetics. The dominant size enlargement mechanism is agglomeration and this assumption is satisfactory.

(2) *The Feed to the Crystallizer is Monodisperse.* The feed PSDs are bell-shaped with narrow standard deviations ($\sigma \leq 2.5\ \mu m$) compared to the product PSD ($\sigma \approx 13\ \mu m$). It follows that the seeds may sensibly be treated as monodisperse.

(3) *The Tracer Particles are Identical to the Feed.* The seed and tracer PSD were both prepared by classification on a Warman Cyclosizer under identical conditions; Ilievski and White (1995) demonstrate that the tracer crystals behave the same as the nontracer crystals during precipitation.

(4) *The Crystallizer Remains at Steady State with Respect to all Variables (and Particularly n) Except for the Distribution of Tracer.* Steady-state operation for these experiments was demonstrated by monitoring the PSD transients Ilievski (1991).

Aggregation is characterized by its rate constant, known as the kernel, β. The frequency with which one particle of size v, aggregates with N of size u, is $\beta(v, u)N$. Many kernels have been proposed for aggregating systems with and without physical justification. For a description of those most frequently applied to crystallizing systems refer to Hartel and Randolph (1986).

The current work is restricted to those kernels amenable to analytical treatment. These are the size-independent kernel $\beta(v, u) = \beta_o$; the sum kernel $\beta(v, u) = \beta_o \times (u + v)$; the product kernel $\beta(v, u) = \beta_o \times u \times v$.

The functional form of a given kernel implies an agglomeration mechanism. In this work, we are investigating the size dependence of the agglomeration kinetics for this system. The derived analytical expressions corresponding to each of these kernels are presented in turn below.

Size-Independent Aggregation of a Monodisperse Feed in MSMPR. The size-independent kernel is frequently found to give a good description, and in many cases the best description of aggregating systems. We may express the extent of aggregation with the parameter $K = N_o \beta_o \tau$. In Appendix A we show that the index of aggregation and K are related by:

$$I_{Agg} = \frac{K + 1 - \sqrt{1 + 2K}}{K} \quad \text{or} \quad K = \frac{2I_{Agg}}{(1 - I_{Agg})^2} \tag{2}$$

The mass density of tracer and the population density are shown in Appendix A to be related by:

$$\frac{\partial M(t, v)}{\partial t} = \beta_o \int_0^v n(t, \epsilon) M(t, v - \epsilon) d\epsilon - \beta_o m_o M - \frac{M}{\tau} \tag{3}$$

The three terms on the righthand side of Eq. 3 are amenable to simple physical explanation. The first term accounts for the production of new tracer particles with $v \in (v, v + dv)$ and every time a particle of mass $v - \epsilon$ aggregates with one of ϵ it adds its mass of tracer to the region $(v, v + dv)$. Unlike the population balance (Eq. A9) no factor of 1/2 is required since we count the mass of tracer in each differential range only once. The second term accounts for loss of tracer from the size range $(v, v + dv)$. Every successful collision between a tracer-bearing particle in that range and any other (whether it bears tracer or not) will remove it from the size range $(v, v + dv)$. The final term is for bulk flow out of the crystallizer.

From Eq. 3 it is deduced that the total mass of tracer varies, as one would expect for a perfectly mixed tank in an exponential fashion:

$$M_T = M_o e^{-t/\tau} \tag{4}$$

Ilievski and White (1995) indeed found that the tracer mass residence time was exponential for the current experiments.

Also from Eq. 3, it can be shown that the tracer mean size varies linearly with time.

$$\frac{\bar{v}_T}{v_o} = 1 + K\frac{t}{\tau} = 1 + \frac{2I_{Agg}}{(1-I_{Agg})^2}\frac{t}{\tau} \tag{5}$$

This last, exceptionally simple, result provides a tool by which the 2-D experimental tracer data may be explored.

Aggregation with the Sum Kernel. This kernel is chosen for analytical convenience, but it also has some physical significance. It is frequently asserted that the rate of aggregation induced by shear is proportional to the cube of the sum of the aggregating particle diameters. Assuming particle mass is proportional to diameter cubed, we have:

$$\beta \propto (u^{1/3} + v^{1/3})^3 = u + 3u^{2/3}v^{1/3} + 3u^{1/3}v^{2/3} + v \geq u + v.$$

So, the sum kernel provides a bound on the behavior of the shear kernel; they are equal when one particle is much larger than the other, but when the particles are of comparable size the sum kernel is substantially smaller.

In the second section of Appendix A, we show that another dimensionless aggregation rate $k = \beta_o \tau N_o v_o$ is related to the index of aggregation by:

$$I_{Agg} = \frac{k}{k+1} \quad \text{or} \quad k = \frac{I_{Agg}}{1-I_{Agg}}$$

The mass density of tracer and the population density are in this instance related by:

$$\frac{\partial M(t,v)}{\partial t} = \beta_o \int_0^v v n(t,\epsilon) M(t, v-\epsilon) d\epsilon - \beta_o (v_o m_o + m_1) M(t,v) - \frac{M(t,v)}{\tau} \tag{6}$$

The total mass of tracer again decays exponentially, as described by Eq. 4.

For the sum kernel, however, the mean tracer size rises exponentially, not linearly as for the size-independent kernel:

$$\frac{\bar{v}_T}{v_o} = \frac{1+2(k-1)e^{kt/\tau}}{2k-1} = \frac{1-I_{Agg}}{3I_{Agg}-1} + \frac{4I_{Agg}-2}{3I_{Agg}-1} \exp\left[\frac{I_{Agg}}{1-I_{Agg}}\frac{t}{\tau}\right] \tag{7}$$

We can see that while this equation is defined for any index of aggregation, it ceases to be meaningful for values in excess of one-third. For a detailed account of this phenomenon, see Smit et al. (1993).

The exponential increase in tracer mean size is a consequence of the fundamental form of the sum kernel that states that large particles aggregate more frequently than do small ones.

Product Kernel. In Appendix A, we characterize aggregation by $\kappa = \beta_o \tau N_o v_o^2$ and deduce that $I_{Agg} = \kappa/2$. We show that the mass density of tracer is related to the size distribution by:

$$\frac{\partial M(t,v)}{\partial t} = \beta_o \int_0^v (v-\epsilon)\epsilon n(t,\epsilon) M(t, v-\epsilon) d\epsilon - \beta_o v m_1 M(t,v) - \frac{M(t,v)}{\tau} \tag{8}$$

from which we deduce that the total mass of tracer decays according to Eq. 4 and that the tracer mean size is given by:

$$\frac{\bar{v}_T}{v_o} = \exp\left[\frac{t}{\tau}\frac{1-\sqrt{1-4\kappa}}{2}\right] = \exp\left[\frac{t}{\tau}\frac{1-\sqrt{1-8I_{Agg}}}{2}\right] \tag{9}$$

As with the sum kernel, the product kernel leads to an exponential increase in tracer mean size. Further, it is valid only for a restricted range of I_{Agg} (in this case $< 1/8$).

Inverse Problem. Muralidar and Ramkrishna (1986) were the first to identify the difficulty of the inverse problem in aggregation. They concluded that if the form of the kernel was to be deduced from particle-size distribution (PSD) data, then that data must be available with improbable precision. For the case in hand, we will now demonstrate the advantages of the tracer data over the PSD data for the identification of the kernel (that is, the agglomeration mechanism).

For a monodisperse feed aggregating in a CST, we show in Appendix B that the size distribution may be calculated as:

$$n(v) = \sum_{i=1}^{\infty} N_i \delta(v - iv_o) \tag{10}$$

From this, we conclude that the number of aggregates containing i seed particles is N_i. The mass of aggregates containing i seed particles is $W_i = \rho v_i N_i$. In Figure 1 we plot a PSD in terms of W_i for the size-independent and sum kernels,

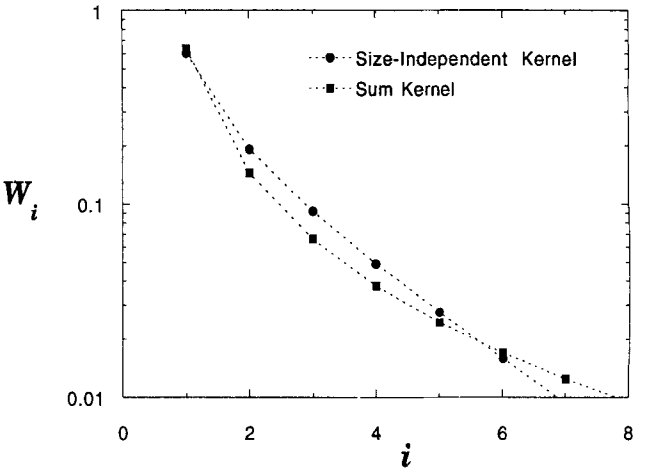

Figure 1. Size distribution for the size-independent and sum kernels, with $I_{Agg} = 1/4$.

Note the difficulty in discriminating between kernels.

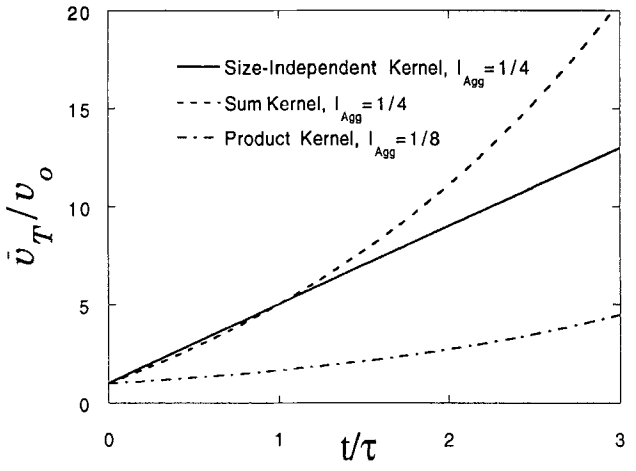

Figure 2. Tracer mean size as a function of kernel type.
Note the ease with which inappropriate forms of the kernel may be rejected.

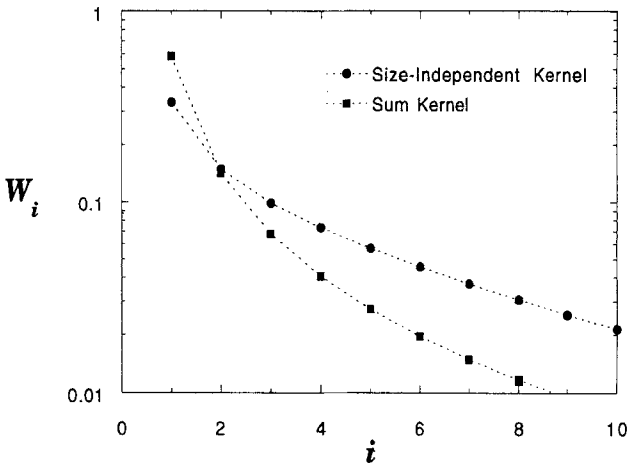

Figure 3. Size distributions corresponding to Figure 2.
Note that it is possible to discriminate between kernels.

with the same index of aggregation, in this case $I_{Agg} = 1/4$. To discriminate between these kernels, we must be able to measure PSD with a high degree of resolution. We are, however, immediately able to exclude the product kernel. As Smit et al. (1993) show, at this value of index of aggregation, with this kernel, the population balance is no longer defined.

As an alternative to fitting kernels to PSD data, in Figure 2 we plot $\bar{v}_T$ for all three kernels considered. The results for the sum and size-independent kernels have been selected so that there is a fivefold increase in $\bar{v}_T$ over one residence time. This corresponds to the experimental results reported later. The result for the product kernel corresponds to the fastest rate of change for which there is a solution, that is, $I_{Agg} = 1/8$. The product kernel is not able to describe a system with a fivefold increase in $\bar{v}_T$ over one residence time. This figure shows that it is much easier to discriminate between kernels using tracer mean size data than from PSD data.

If we combine these two approaches, that of PSD-fitting and tracer-mean-size fitting, we have an even more powerful technique for discriminating between kernels. The $\bar{v}_T$ curves in Figure 2 correspond to values of $K = 4$, $k = 0.424$, and $\kappa = 1/4$. These in turn correspond to indices of aggregation of 0.5, 0.298, and 0.125 for the size-independent, sum and product kernels, respectively. These estimates of I_{Agg} from fits to the tracer data may then be compared with the observed values of I_{Agg}, and the kernels thus discriminated. However, it is not always possible, or can be very difficult, to obtain a reliable estimate of I_{Agg}, such as when substantial fines are present. In such cases, we may compare the experimental PSD with simulated PSDs generated from the parameters of the fit to the tracer data. Figure 3 shows the PSDs for the size-independent and sum kernels corresponding to the $\bar{v}_T$ curves of Figure 2. In summary our proposed technique for discriminating between kernels is as follows:

(1) Collect the following experimental data: steady-state PSD and, if possible, I_{Agg}; pulse-response tracer mean size.

(2) Fit the $\bar{v}_T - t$ curves to the experimental data for each of the kernels under consideration. Reject those kernels not capable of describing the data. At present, this stage is limited to the three kernels amenable to analytical treatment, giving rise to Eqs. 5, 7, and 9.

(3) Estimate the indices of aggregation corresponding to the $\bar{v}_T - t$ curve fit. If possible, compare the I_{Agg} values with the experimental data and reject or accept kernels.

(4) Calculate the product-size distributions corresponding to the values of I_{Agg} calculated above. Compare these with the experimental data and accept or reject kernels.

In the next section we apply this technique to our data for the $Al(OH)_3$ system.

Tracer data analysis

Quantitative Tracer Data. The quantities measured during the tracer experiments are: (1) M_i, the mass of tracer in the ith sieve-size range, at time t, and (2) $n(L)$, the crystal-size number density distribution at steady state. These measured quantities can be related to the results of the theoretical analysis. The mass of tracer in the ith sieve size fraction, at time t, is:

$$M_i(t) = \int_{v_i}^{v_{i+1}} \int_0^{v_{i+1}} c f(t, v, c) dc dv \tag{11}$$

The mean volume size of the tracer mass distribution is estimated from the tracer data by:

$$\bar{v}_T(t) = \frac{\sum_i \bar{v}_i M_i}{\sum_i M_i} \tag{12}$$

The average particle volume in the ith size interval, $\bar{v}_i$, is estimated from the sieve interval geometric mean size, $L_{s,i}$, by:

$$\bar{v}_i = 0.7 L_{s,i}^3$$

This relationship was obtained using the measured-size distributions from a sieve analysis and from the Elzone Calloscope 280PCXY, Allen (1990).

Agglomeration Mechanism Identification. A number of agglomeration kernels have been proposed in the literature for the agglomeration of $Al(OH)_3$ during precipitation in a stirred crystallizer. From theoretical considerations, Low (1975) proposes a size-dependent, diffusional turbulence kernel. In contrast, Halfon and Kaliaguine (1976) assumed the *random coalescence* mechanism (size-independent kernel), all particles having an equal probability of agglomerating. Using this kernel they were able to fit their batch $Al(OH)_3$ precipitation data. Ilievski and White (1994) concluded that batch agglomeration in this system is by random coalescence. This conclusion was drawn from two independent results. First, the shape of the experimentally obtained *self-preserving* PSD, for this system, was consistent with the size-independent agglomeration kernel. Secondly, a statistical comparison of the quality of the fit to the experimental PSD data of a number of agglomeration kernels, including the Low (1975) kernel, showed the size-independent kernel to give consistently better agreement with the data.

Following the kernel discrimination procedure outlined earlier, we can immediately dismiss the product kernel, as it does not give a realistic solution at the observed values of I_{Agg}. Figures 4a, 4b, and 4c show the experimental mean volume size of the tracer mass distribution, $\bar{v}_T$, plotted as a dimensionless quantity against time, for each experiment. v_0 is estimated by linear extrapolation of the tracer mean to time $t = 0$. Also presented in these plots are the fitted curves corresponding to the size-independent and sum kernel mechanisms, as described by Eqs. 5 and 7, respectively. The error bars show only the uncertainty introduced into estimates of $\bar{v}_T$ because discretized data (sieve size intervals) were used rather than continuous data, refer to Appendix C. As can be seen from the figures, the shapes of the fitted size-independent and sum kernel equations are both consistent with experimental $\bar{v}_T$ data. However, a comparison between the experimentally observed values of I_{Agg} and those values estimated from the parameters of the curve fit, presented in Table 2, shows there is a difference between the kernels. The size-independent can be seen to agree better with the data.

Figures 5a, 5b and 5c show the same information plotted another way. Plotted here, alongside the experimental $\bar{v}_T$, are the predicted size-independent and sum kernel models using the experimentally obtained values of I_{Agg}. These figures clearly support the choice of the size-independent agglomeration model over the sum kernel. In fact, Figure 5c shows a case where the sum kernel is incapable of describing the form of the tracer data. Estimates of the magnitude of β_o can be obtained from the tracer data using Eq. 5.

The above conclusion agrees with the findings of Ilievski and White (1994) who deduce their results from the study of *batch* precipitation, rather than from *continuous* experiments as reported here.

It is uncertain why the size-independent kernel best fits the available agglomeration data for this system. Further, the size-independent kernel has been shown by Hounslow (1990) to be satisfactory for modeling the agglomeration of calcium oxalate during precipitation in an agitated vessel. It is possible that under the present experimental conditions the size-independent kernel is a manifestation of Smoluchowski's Brownian kernel (1917) with a aggregation effectiveness term, ψ, for which

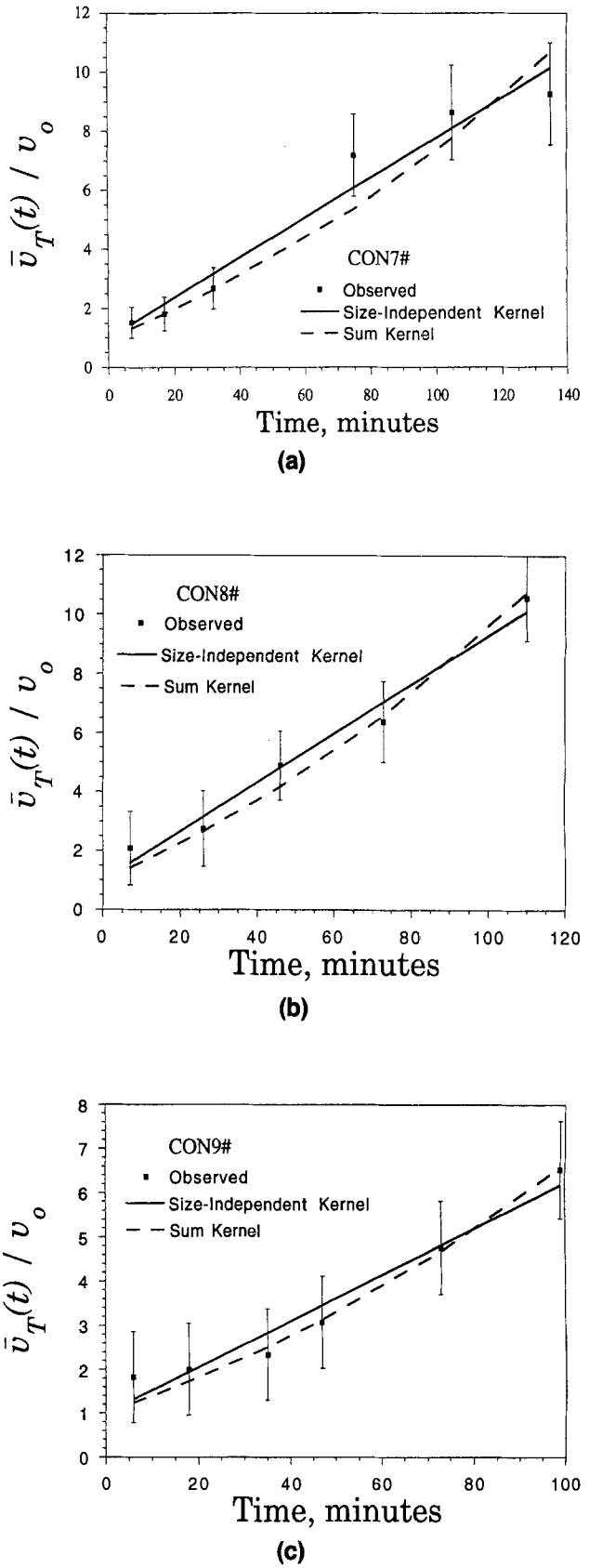

Figure 4. Least-squares fits to the experimental tracer data.

Con7# (a); Con8# (b); Con9# (c).

Table 2. Comparison of I_{Agg} Values

Run No.	Observed I_{Agg}	I_{Agg} Estimated from Curve Fits	
		Size-Independent	Sum Kernel
Con7#	0.53±0.04	0.52	0.29
Con8#	0.56±0.04	0.53	0.30
Con9#	0.44±0.03	0.42	0.27

$$\beta(v, u) = \psi\frac{8}{3}\frac{kT}{\mu}\left(\frac{1}{u^{1/3}} + \frac{1}{v^{1/3}}\right)(u^{1/3} + v^{1/3}) \approx \psi\frac{8}{3}\frac{kT}{\mu}$$

where k here is the Boltzman constant, T is absolute temperature, and μ is the viscosity.

Alternatively, while a size-dependent kernel may better describe the aggregate collision process, the overall process of forming a strong measurable agglomerate may be better described by the size-independent kernel. This overall agglomeration process is the sum of a number of subprocesses, that is, particle collision, aggregation, the rupture of flocs or aggregates of varying strength, and a cementation process that bonds the aggregate. Recently, a further possible explanation was advanced in another article from our group, Smit et al. (1993). They demonstrate that the population balance model for agglomeration breaks down when used with many of the theoretically developed agglomeration kernels in a manner analogous to the failure of the product kernel in the current study.

Conclusions

The Zn-doped $Al(OH)_3$ tracer crystals have been demonstrated to be a useful tool for the quantitative investigation of agglomeration behavior during precipitation.

A 2-D population balance technique is presented which aids discrimination between agglomeration kernels and enables estimates of the agglomeration kinetics to be made. An algorithm, incorporating this technique, is shown to be a powerful tool for discriminating between kernels.

Three agglomeration kernels were considered. For the continuous precipitation of $Al(OH)_3$, only the size-independent kernel was found to be consistent with the experimental data. This result agrees with the findings of Ilievski and White (1994) obtained from batch precipitation studies.

Estimates of the agglomeration parameters (such as I_{Agg} and β_o) from the tracer data are in good agreement with the experimentally observed values.

Acknowledgment

The authors gratefully acknowledge the support of CSIRO Australia and the Science and Engineering Research Council of Great Britain under its Specially Promoted Programme in Particle Technology. Thanks are due to Comalco R&D Laboratory, Thomastown, Australia, for funding the data collection through a PhD program.

Notation

c = mass of Zn per tracer particle
$f(t, v, c)$ = tracer density distribution
$k = \beta_o \tau N_o v_o$
L_{30} = volume mean size of a size distribution

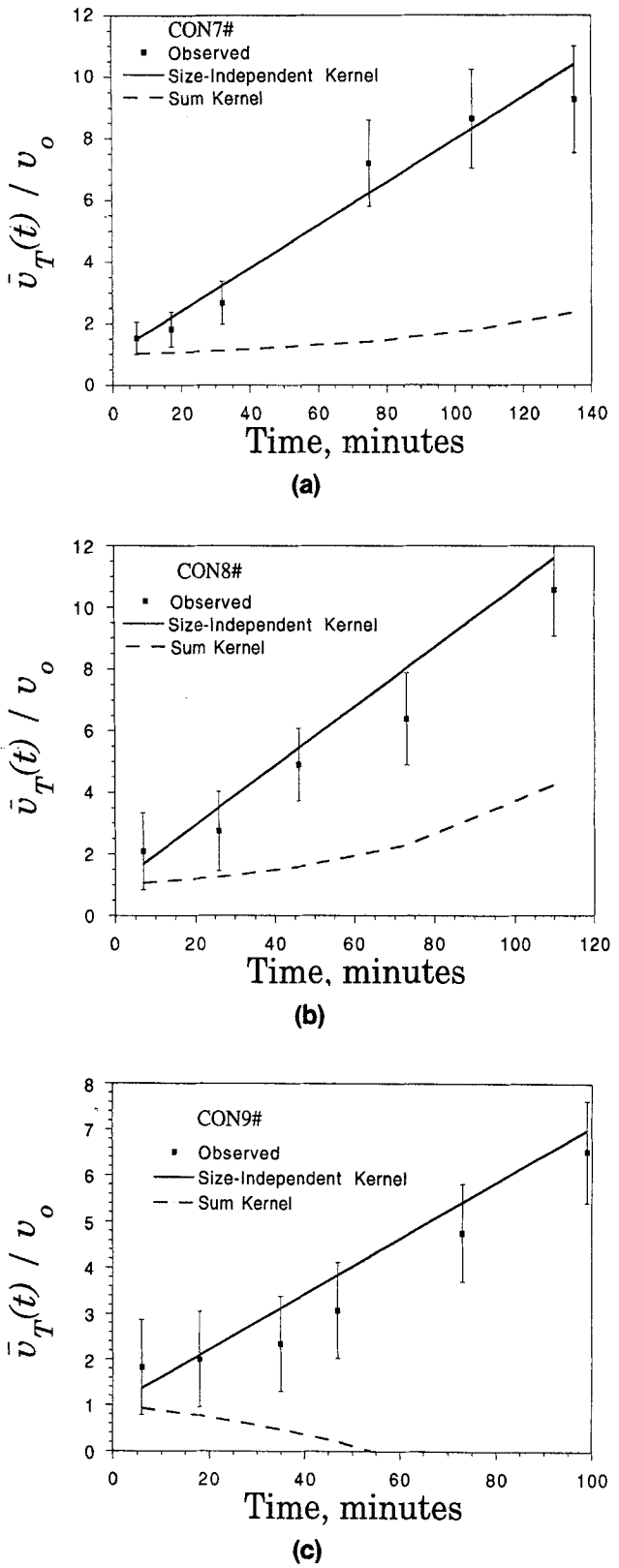

Figure 5. Predicted tracer mean sizes from the size-independent and sum kernel models, using the observed values of I_{Agg}.

Con7# (a); Con8# (b); Con9# (c).

$L_{s,i}$ = geometric mean size of the ith sieve size interval, μm
M_T = total mass of tracer per unit volume of suspension
$n(v)$ = number-volume density function
N_o = number of seed particles in the crystallizer, No./mL
N_t = total number at steady state, No./mL
S = supersaturation ratio as the supersaturation in Al (as g/L Al_2O_3) over the caustic concentration (as g/l Na_2O)
v_o = seed particle volume, μm^3
$\bar{v}_i$ = average particle volume in the ith size interval, μm^3
$\bar{v}_T(t)$ = mean volume size of the tracer mass distribution, μm^3
v, u = variable volume, μm^3

Greek letters

$\beta(v,u)$ = agglomeration kernel
$\kappa = \beta_0 \tau N_0 v_0^2$
σ = standard deviation of a size distribution
τ = mean residence time, min.

Subscript

i = pertaining to the ith size interval

Literature Cited

Allen, T., *Particles Size Measurement*, 4th ed., Chapman and Hall, London (1990).

Halfon, A., and S. Kaliaguine, "Alumina Trihydrate Crystallisation: 2. A Model of Agglomeration," *Can. J. of Chem. Eng.*, **54**, 168 (1976).

Hartel, R. W., and A. D. Randolph, "Mechanisms and Kinetic Modelling of Calcium Oxalate Crystal Aggregation in Urine-Like Liquors: 2. Kinetic Modelling," *AIChE J.*, **32**(7), 1186 (1986).

Hounslow, M. J., "A Discretized Population Balance for Nucleation, Growth and Aggregation," PhD Thesis, Univ. of Adelaide, Australia (1990).

Ilievski, D., "Modelling $Al(OH)_3$ Agglomeration During Batch and Continuous Precipitation in Supersaturated Caustic Aluminate Solutions," PhD Thesis, Univ. of Queensland (1991).

Ilievski, D., and E. T. White, "Agglomeration During Precipitation: Agglomeration Mechanism Identification for $Al(OH)_3$ Crystals in Stirred Caustic Aluminate Solution," *Chem. Eng. Sci.*, **49**(19), 3227 (1994).

Ilievski, D., and E. T. White, "Agglomeration During Precipitation: I. Tracer Crystals for $Al(OH)_3$ Precipitation," *AIChE J.*, **41**, 518 (1995).

Low, G. C., "Agglomeration Effects in Aluminium Trihydroxide Precipitation," PhD Thesis, Univ. of Queensland (1975).

Muralidar, R., and D. Ramkrishna, "An Inverse Problem in Agglomeration Kinetics," *J. Colloid Interf. Sci.*, **112**, 348 (1986).

Randolph, A. D., and M. A. Larson, *Theory of Particulate Processes*, 2nd ed., Academic Press, New York (1988).

Smit, D., M. J. Hounslow, and W. R. Paterson, "Aggregation and Gelation: I. Analytical Solutions for CST and Batch Operation," *Chem. Eng. Sci.*, **49**, 1025 (1994).

Smoluchowski, M. V., "Versuch einer Mathematischen Theorie der Koagulationskinetik Kolloider Lösungen," *Z. Phys. Chem.*, **92**, 129 (1917).

Wolfram, S., *Mathematica*, 2nd ed., Addison-Wesley, Redwood City, (1991).

Appendix A: Two-Dimensional Population Balance

Define the two-dimensional population density function $f(t, v, c)$ so that the number of particles, per unit volume of suspension, with mass $v \in (v, v + dv)$ and tracer mass $c \in (c, c + dc)$ is $dN = f dv dc$. The variable, v, may be interpreted as volume if the crystal densities are uniform with size.

Moments

We can define a variety of 1-D and 2-D moments. The general 2-D moment is:

$$m_{i,j}(t) = \int_0^\infty \int_0^v v^i c^j f(t, v, c) dc dv \tag{A1}$$

A useful 1-D moment of the distribution of tracer at a given size is:

$$\mu_j(t, v) = \int_0^v c^j f(t, v, c) dc \tag{A2}$$

This moment can be used to calculate two measurable 1-D size distributions: $n(t, v)$ the conventional population density, relating the number density of particles to their total size, and $M(t, v)$ the mass density of tracer.

$$n(t, v) = \int_0^v f(t, v, c) dc = \mu_0(t, v) \tag{A3}$$

$$M(t, v) = \int_0^v c f(t, v, c) dc = \mu_1(t, v) \tag{A4}$$

It is also possible to calculate the moments of M.

$$\int_0^\infty v^i M dv = \int_0^\infty \int_0^v v^i c f dc dv = m_{i,1} \tag{A5}$$

Of particular interest to us is the total mass of tracer present:

$$M_T(t) = \int_0^\infty M dv = m_{0,1}(t) \tag{A6}$$

and the mean of M:

$$\bar{v}_T(t) = \frac{\int_0^\infty v M dv}{\int_0^\infty M dv} = \frac{m_{1,1}(t)}{m_{0,1}(t)} \tag{A7}$$

The conventional moments of a size distribution may be deduced by integrating over all tracer masses:

$$m_i(t) = \int_0^\infty v^i n(t, v) dv = \int_0^\infty \int_0^v v^i f(t, v, c) dc dv = m_{i,0} \tag{A8}$$

Size-independent aggregation of a monodisperse feed in a CST

We turn now to the analysis of an idealized representation of the experimental system. We employ the assumptions identified earlier in the theory section.

The conventional population balance for aggregation in a CST at steady state is given by Randolph and Larson (1988) as:

$$\frac{n - n^{in}}{\tau} = \frac{\beta_0}{2} \int_0^v n(v - \epsilon) n(\epsilon) d\epsilon - \beta_0 n(v) \int_0^\infty n(\epsilon) d\epsilon \tag{A9}$$

The feed consists of N_o particles per unit volume of size v_o. So $n^{in} = N_o \delta(v - v_o)$.

We take the Laplace transform of the population balance with respect to particle mass yielding, after some simplification:

$$\tilde{n}(s) = \frac{N_o}{K}[\sqrt{1+2K} - \sqrt{1+2K(1-e^{-v_o s})}] \quad \text{(A10)}$$

where $K = N_o \beta_o \tau$. In Appendix B we deduce the inverse of this transform. However, the s-domain result is sufficient for our purposes at the moment. In this form it can be used as a moment generating function, since:

$$m_i = \lim_{s \to 0} (-1)^i \frac{d^i \tilde{n}(s)}{ds^i} \quad \text{(A11)}$$

So, $m_o = N_t = N_o/K(\sqrt{1+2K} - 1)$, and therefore, the index of aggregation:

$$I_{Agg} = 1 - \frac{N_t}{N_o} = \frac{K + 1 - \sqrt{1+2K}}{K} \quad \text{or } K = \frac{2I_{Agg}}{(1-I_{Agg})^2} \quad \text{(A12)}$$

Distribution of Tracer by Size. The dynamic 2-D population balance for this system is:

$$\frac{\partial f}{\partial t} = B - D - \frac{f}{\tau} \quad \text{(A13)}$$

where

$$B(t, v, c) = \frac{\beta_o}{2} \int_0^v \int_0^c f(t, v-\epsilon, c-\gamma) f(t, \epsilon, \gamma) d\gamma d\epsilon \quad \text{(A14)}$$

$$D(t, v, c) = \beta_o f(t, v, c) \int_0^\infty \int_0^v f(t, \epsilon, \gamma) d\gamma d\epsilon = \beta_o f m_o \quad \text{(A15)}$$

We are able to neglect the term for flow into the system as we are dealing with pulse responses. The magnitude of the pulse is accounted for in the initial condition introduced after Eq. A20.

We may take 1-D moments with respect to tracer mass to give:

$$\frac{\partial \mu_j(t, v)}{\partial t} = \bar{B}_j(t, v) - \bar{D}_j(t, v) - \frac{\mu_j(t, v)}{\tau} \quad \text{(A16)}$$

where

$$\bar{B}_j(t, v) = \frac{\beta_o}{2} \int_0^\infty \int_0^v \int_0^c c^j f(t, v-\epsilon, c-\gamma) f(t, \epsilon, \gamma) d\gamma d\epsilon dc \quad \text{(A17)}$$

$$\bar{D}_j(t, v) = \beta_o \int_0^\infty c^j f(t, v, c) \int_0^\infty \int_0^v f(t, \epsilon, \gamma) d\gamma d\epsilon dc = \beta_o m_o \mu_j \quad \text{(A18)}$$

Our particular concern is with the first moment. For this case ($j = 1$) (Eqs. A16–A18) become:

$$\frac{\partial \mu_1(t, v)}{\partial t} = \beta_o \int_0^\infty \mu_o(t, \epsilon) \mu_1(t, v-\epsilon) d\epsilon - \beta_o m_o \mu_1 - \frac{\mu_1}{\tau} \quad \text{(A19)}$$

However, by Eqs. A3 and A4 μ_0 and μ_1 are n and M, respectively. We may now write an equation describing how the tracer mass is distributed by time and size:

$$\frac{\partial M(t, v)}{\partial t} = \beta_o \int_0^v n(t, \epsilon) M(t, v-\epsilon) d\epsilon - \beta_o m_o M - \frac{M}{\tau} \quad \text{(A20)}$$

subject to the initial condition $M(0, v) = M_o \delta(v - v_o)$.

Once again we take the Laplace transform with respect to particle mass, yielding:

$$\frac{\partial \tilde{M}(t, s)}{\partial t} = \beta_o \tilde{n} \tilde{M} - \beta_o m_o \tilde{M} - \frac{\tilde{M}}{\tau} \quad \text{(A21)}$$

We have assumed that n is independent of time, so this first-order ODE can be solved:

$$\ln\left[\frac{\tilde{M}(t, s)}{\tilde{M}(0, s)}\right] = \frac{t}{\tau}(\beta_o \tau \tilde{n} - \beta_o \tau m_o - 1) \quad \text{(A22)}$$

If we combine this with the result for $\tilde{n}$, (Eq. A10), we obtain:

$$\tilde{M}(t, s) = M_o \exp\left[-v_o s - \frac{t}{\tau}\sqrt{1+2K(1-e^{-v_o s})}\right] \quad \text{(A23)}$$

As before, we can use this result to obtain the moments of M:

$$m_{i,1}(t) = \lim_{s \to 0} (-1)^i \frac{\partial^i \tilde{M}(t, s)}{\partial s^i} \quad \text{(A24)}$$

So, the total mass of tracer per unit volume is:

$$M_T = m_{1,0} = \tilde{M}(t, 0) = M_0 e^{-t/\tau} \quad \text{(A25)}$$

We may also calculate the tracer mean size:

$$\bar{v}_T = \frac{m_{1,1}}{m_{0,1}} = \frac{-\bar{M}'(0)}{\tilde{M}(0)} = v_0\left(1 + K\frac{t}{\tau}\right) \quad \text{(A26)}$$

In dimensionless form it is:

$$\frac{\bar{v}_T}{v_0} = 1 + K\frac{t}{\tau} = 1 + \frac{2I_{Agg}}{(1-I_{Agg})^2}\frac{t}{\tau} \quad \text{(A27)}$$

Aggregation with the sum kernel

The population balance is:

$$\frac{n-n^{in}}{\tau}=\frac{\beta_o}{2}\int_0^{v} vn(v-\epsilon)n(\epsilon)d\epsilon - \beta_0 n(v)\int_0^{\infty}(v+\epsilon)n(\epsilon)d\epsilon \quad \text{(A28)}$$

Proceeding as before, we next take the Laplace transform:

$$\frac{\tilde{n}-N_o\epsilon^{-v_o s}}{\tau}=-\beta_o\tilde{n}\frac{d\tilde{n}}{ds}-\beta_o\left(m_1\tilde{n}-m_o\frac{d\tilde{n}}{ds}\right) \quad \text{(A29)}$$

When dealing with size-independent aggregation, the corresponding equation, (Eq. A10), was explicit in $\tilde{n}$, whereas Eq. A29 is a nonlinear, nonhomogeneous ODE. In Appendix B we develop a series solution for $\tilde{n}$, but at this stage we wish to know $\tilde{n}(0)$, $\tilde{n}'(0)$, and so on.

We proceed as follows. We can develop without difficulty a Taylor series, about $s=0$, equivalent to Eq. A29. The coefficients of that series will involve in the normal way the derivatives of $\tilde{n}$ at $s=0$—precisely the quantities desired. These may then be determined by equating coefficients of s.

The Taylor series equivalent of Eq. 29 is:

$$-N_o+\tilde{n}(0)-\beta_o\tau\tilde{n}(0)\tilde{n}'(0)+[N_o v_o+\tilde{n}'(0)]s + \left[\frac{\tilde{n}''(0)-N_o v_o^2}{2}+\beta_o\tau\tilde{n}'(0)\tilde{n}''(0)\right]s^2+O(s^3)=0 \quad \text{(A30)}$$

Since each of the coefficients in this polynomial must be zero, we can develop three simultaneous equations in terms of $\tilde{n}(0)$, $\tilde{n}'(0)$, and so on. These in turn yield the moments:

$$m_o=N_t=\frac{N_o}{1+k} \quad m_1=N_o v_o \quad m_2=\frac{N_o v_o^2}{1+2k} \quad \text{(A31)}$$

where $k=\beta_o\tau N_o v_o$. We observe, therefore, that $I_{Agg}=k/(k+1)$ so that complete aggregation occurs as $k\to\infty$. We note also that the first moment, or total mass per unit volume, is independent of k.

Distribution of Tracer by Size with the Sum Kernel. We again apply Eq. A13, but with:

$$B(t,v,c)=\frac{\beta_o}{2}\int_0^{v}\int_0^{c} vf(t,v-\epsilon,c-\gamma)f(t,\epsilon,\gamma)d\gamma d\epsilon \quad \text{(A32)}$$

$$D(t,v,c)=\beta_o f(t,v,c)\int_0^{\infty}\int_0^{v}(v+\epsilon)f(t,\epsilon,\gamma)d\gamma d\epsilon = \beta_o(vm_o+m_1)f \quad \text{(A33)}$$

So, rather than Eq. 20 we have:

$$\frac{\partial M(t,v)}{\partial t}=\beta_o\int_0^{v} vn(t,\epsilon)M(t,v-\epsilon)d\epsilon - \beta_o(v_o m_o+m_1)M(t,v)-\frac{M(t,v)}{\tau} \quad \text{(A34)}$$

The Laplace transform of this equation is:

$$\frac{\partial\tilde{M}(t,s)}{\partial t}=\beta_o\left[-\tilde{n}(t,s)\frac{\partial\tilde{M}(t,s)}{\partial s}-\tilde{M}(t,s)\frac{\partial\tilde{n}(t,s)}{\partial s} + m_o-m_1\tilde{M}(t,s)\right]-\frac{\tilde{M}(t,s)}{\tau} \quad \text{(A35)}$$

Yet again, we have no expectation of solving this ODE let alone inverting the transform. Instead, we will be content with determining $\tilde{M}(0)=m_{0,1}$ and $\tilde{M}'(0)=m_{1,1}$. We do so by again taking the Taylor series, combining with Eq. A30, and equating coefficients. This yields:

$$\frac{dm_{0,1}}{dt}+\frac{m_{0,1}}{\tau}=0 \quad \frac{dm_{1,1}}{dt}+\frac{m_{1,1}}{\tau}+\frac{k}{\tau}\left(\frac{v_o m_{0,1}}{1-2k}-m_{1,1}\right)=0 \quad \text{(A36)}$$

This pair of first-order ODEs may be solved to give:

$$m_{0,1}(t)=m_{0,1}(0)e^{-t/\tau} \quad \text{(A37)}$$

$$m_{1,1}(t)=m_{1,1}(0)\frac{e^{-t/\tau}+2(k-1)e^{(k-1)t/\tau}}{2k-1} \quad \text{(A38)}$$

Finally, the total mass of tracer and the mean size may be calculated:

$$M_T=m_{0,1}=M_o e^{-t/\tau} \quad \text{(A39)}$$

$$\bar{v}_T=\frac{m_{1,1}}{m_{0,1}}=v_0\frac{1+2(k-1)e^{kt/\tau}}{2k-1} \quad \text{(A40)}$$

In terms of the index of aggregation, this last result is:

$$\frac{\bar{v}_T}{v_0}=\frac{1-I_{Agg}}{3I_{Agg}-1}+\frac{4I_{Agg}-2}{3I_{Agg}-1}\exp\left[\frac{I_{Agg}}{1-I_{Agg}}\frac{t}{\tau}\right] \quad \text{(A41)}$$

Product kernel

We proceed with this kernel exactly as we did with the sum kernel. The population balance is now:

$$\frac{n-n^{in}}{\tau}=\frac{\beta_0}{2}\int_0^{v}(v-\epsilon)\epsilon n(v-\epsilon)n(\epsilon)d\epsilon - \beta_o v n(v)\int_0^{\infty}\epsilon n(\epsilon)d\epsilon \quad \text{(A42)}$$

Or, in the Laplace domain:

$$\frac{\tilde{n}-N_o e^{-v_o s}}{\tau}=\frac{\beta_o}{2}\left(\frac{d\tilde{n}}{ds}\right)^2+\beta_o m_1\frac{d\tilde{n}}{ds} \quad \text{(A43)}$$

By means of a Taylor series expansion the moments may be deduced:

$$m_o = N_t = N_o\left(1-\frac{\kappa}{2}\right) \quad m_1 = N_o v_o \quad m_2 = N_o v_o^2 \frac{1-\sqrt{1-4\kappa}}{2\kappa} \tag{A44}$$

where $\kappa = \beta_o \tau N_o v_o^2$. We observe, therefore, that $I_{Agg} = \kappa/2$ so that complete aggregation occurs as $\kappa \to 2$. We note also that the first moment, or total mass per unit volume, is independent of κ.

Distribution of Tracer by Size with the Product Kernel. We again apply Eq. A13, with:

$$B(t, v, c) = \frac{\beta_o}{2}\int_0^v \int_0^c (v-\epsilon)\epsilon f(t, v-\epsilon, c-\gamma) \times f(t, \epsilon, \gamma) d\gamma d\epsilon \tag{A45}$$

$$D(t, v, c) = \beta_o f(t, v, c)\int_0^\infty \int_0^v v\epsilon f(t, \epsilon, \gamma) d\gamma d\epsilon = \beta_o v f m_1 \tag{A46}$$

So, rather than Eq. A20 we have:

$$\frac{\partial M(t, v)}{\partial t} = \beta_o \int_0^v (v-\epsilon)\epsilon n(t, \epsilon) M(t, v-\epsilon) d\epsilon - \beta_0 v m_1 M(t, v) - \frac{M(t, v)}{\tau} \tag{A47}$$

The Laplace transform of this equation is:

$$\frac{\partial \tilde{M}(t, s)}{\partial t} = \beta_o \frac{\partial \tilde{M}(t, s)}{\partial s}\left(\frac{\partial \tilde{n}(t, s)}{\partial s} + m_1\right) - \frac{\tilde{M}(t, s)}{\tau} \tag{A48}$$

We can extract the moments of M from a Taylor series expansion, to give:

$$\frac{dm_{0,1}}{dt} + \frac{m_{0,1}}{\tau} = 0 \quad \frac{dm_{1,1}}{dt} + \frac{m_{1,1}}{2\tau}(1+\sqrt{1-4\kappa}) = 0 \tag{A49}$$

This pair of first-order ODEs may be solved to give the total mass of tracer and the mean size:

$$M_T = m_{0,1} = M_0 e^{-t/\tau} \tag{A50}$$

$$\bar{v}_T = \frac{m_{1,1}}{m_{0,1}} = v_o \exp\left[\frac{t}{\tau}\frac{1-\sqrt{1-4\kappa}}{2}\right] = v_o \exp\left[\frac{t}{\tau}\frac{1-\sqrt{1-8I_{Agg}}}{2}\right] \tag{A51}$$

Appendix B: Series Solutions for Population Density Function

We seek solutions to the population balance equation by means of series expansions in the Laplace domain.

Size-independent kernel

We may expand Eq. A10 in powers of $e^{-v_o s}$ to give:

$$\frac{\tilde{n}(s)}{N_o} = \frac{e^{-v_o s}}{(1+2K)^{1/2}} + \frac{Ke^{-2v_o s}}{2(1+2K)^{3/2}} + \frac{k^2 e^{-3v_o s}}{2(1+2K)^{5/2}} + \frac{5k^3 e^{-4v_o s}}{8(1+2K)^{7/2}} + \ldots = \sum_{i=1}^{\infty} C_i e^{-iv_o s} \tag{B1}$$

where

$$C_i = \frac{K^{i-1}}{(1+2K)^{i-1/2}} \frac{1\times1\times3\times5\times7\times\ldots\times(2i-3)}{i!} = -\frac{K^{i-1}}{(1+2K)^{i-1/2}} \prod_{j=1}^{i}\left(2-\frac{3}{j}\right) \tag{B2}$$

We may invert Eq. B1 to give the population density as a series of impulses at integer multiples of the seed size:

$$n(v) = N_o \sum_{i=1}^{\infty} C_i \delta(v - iv_o) = \sum_{i=1}^{\infty} N_i \delta(v - iv_0) \tag{B3}$$

This result makes it clear that since all aggregates are made up of an integer number of seed particles, each of mass v_o, that the aggregates themselves must have a mass that is an integer multiple of the seed mass. By means of Eq. B2 we may calculate the number of aggregates, N_i, containing i seed particles.

Sum and product kernels

Equations A29 and A43 differ from Eq. A10 in that they are (nonlinear) differential equations in s, rather than explicit algebraic equations. We adopt the following approach.

(1) Transform variables so that $y(x) = \tilde{n}(s)/N_o$ when $x = e^{-v_o s}$. For example, Eq. A29 becomes:

$$\frac{y-x}{k} = xyy' - y - \frac{xy'}{1+k} \tag{B4}$$

(2) Develop a Taylor series for Eq. B4 in terms of $y = \Sigma C_i x^i$. Solve for the C_i, numerically, in the manner of Wolfram (1991). As previously, the number of aggregates containing i seed particles is $N_i = N_o C_i$.

The algebraic forms of the C_i depend on the length of the expansion of Eq. B4. However, by considering expansions of various lengths, numerically converged solutions were obtained for specific values of k.

Appendix C: Discretization Error in Tracer Distribution

Here we develop an expression for the error introduced into estimates of $\bar{v}_T$ that results from using the discretized mass-tracer distribution (histogram) in Eq. 12. The discretiza-

tion is a consequence of splitting the tracer samples into finite-size intervals. This analysis ignores experimental error, which would be in addition to the discretization error.

The definition of $\bar{v}_T$ is:

$$\bar{v}_T(t) = \frac{\int_0^\infty vMdv}{\int_0^\infty Mdv} = \int_0^\infty v\hat{M}(v)dv \tag{A7}$$

$\bar{v}_T$ is estimated from the experimental data by:

$$\bar{v}_T(t) = \sum_{i=1}^{n} \bar{v}_i \frac{M_i}{\sum_i M_i} = \sum_{i=1}^{n} \bar{v}_i \hat{M}_i \tag{12}$$

The error introduced by discretization of the distribution into n intervals is:

$$\epsilon = \int_0^\infty v\hat{M}(v)dv - \sum_{i=1}^{n} \bar{v}_i \hat{M}_i$$

if $v_n > v^*$, $\hat{M}(v^*) = 0$

$$\epsilon = \sum_{i=1}^{n} \int_{v_i}^{v_{i+1}} v\hat{M}(v)dv - \sum_{i=1}^{n} \bar{v}_i \hat{M}_i$$

Then for the ith interval:

$$\epsilon_i = \int_{v_i}^{v_{i+1}} v\hat{M}(v)dv - \bar{v}_i \hat{M}_i = \int_{v_i}^{v_{i+1}} v\hat{M}(v)dv - \bar{v}_i[F_{i+1} - F_i] \tag{C1}$$

where $F_i = F(v_i)$, the cumulative distribution of $\hat{M}(v) = dF(v)/dv$, at v_i and:

$$\epsilon = \sum_{i=1}^{n} \epsilon_i$$

The integral in Eq. C1 is evaluated using integration by parts and by a Taylor expansion about $\bar{v}_i$. For simplicity we have taken $\bar{v}_i = (v_{i+1} + v_i)/2$, and define $h_i = v_{i+1} - v_i$. The first-order approximation from the Taylor expansion is:

$$\epsilon_i = \frac{h_i}{2}[F_{i+1} - F_i].$$

Manuscript received Oct. 29, 1993, and revision received Mar. 30, 1994.